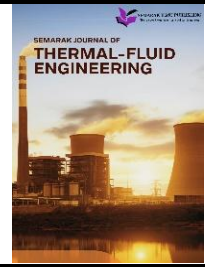




Semarak Journal of Thermal-Fluid Engineering

Journal homepage:
<https://semarakilmu.com.my/journals/index.php/sjotfe/index>
ISSN: 3030-6639



Modeling of the External Airflow in Mountain with Different Velocity and Turbulence Models

Muhamad Luqman Mohd Zabidy, Muhammad Rafiuddin Ekhwann^{1,*}, Muhammad Syamil¹

¹ Department of Mechanical Engineering and Manufacturing, University Tun Hussein Onn, Parit Raja, 86400, Johor, Malaysia

ARTICLE INFO

Article history:

Received 19 April 2025

Received in revised form 11 May 2025

Accepted 22 May 2025

Available online 26 June 2025

Keywords:

External airflow; heat transfer; wind velocity; turbulence model; mountain terrain; computational fluid dynamics (CFD)

ABSTRACT

This study investigates external airflow and heat transfer over mountainous terrain using computational fluid dynamics (CFD) simulations, considering varying wind velocities and turbulence models. The research incorporates boundary conditions with wind velocities of 50 m/s, 100 m/s, and 150 m/s while implementing turbulence models such as k-epsilon, k-omega SST, and k-kl-omega. A computational domain replicating real-world topographical features with high-resolution meshing ensures accurate simulations. The study evaluates airflow separation, turbulence formation, and heat dissipation across the mountain surface. Results indicate that at low wind velocities, heat remains concentrated near the surface, whereas higher velocities enhance convective effects, improving heat dissipation and reducing surface temperatures. Among turbulence models, the k-omega SST and k-kl-omega models exhibited superior accuracy in predicting temperature gradients. The lowest recorded surface temperature was 25.2256°C for the k-kl-omega model at 150 m/s, demonstrating efficient cooling effects. The study also conducted a grid independence test, confirming that an optimal element size of 40 mm provided the most reliable results, with an average mountain surface temperature of 1200.02°C, ensuring accurate modeling of wind interactions. Additionally, the airflow behavior was analyzed to assess turbulence intensity, recirculation zones, and pressure variations, which are critical for wind energy optimization and infrastructure planning. These findings highlight the importance of selecting appropriate turbulence models and boundary conditions for improving wind farm efficiency, environmental monitoring, and climate adaptation strategies. CFD proves to be a valuable tool for predicting complex airflow behaviors in mountainous terrains, aiding in sustainable energy solutions and thermal management. The study concludes that precise modeling of external airflow enhances the understanding of aerodynamic and thermal interactions, supporting renewable energy applications and infrastructure development in complex terrains.

1. Introduction

Mountainous regions, with their varied terrain and major effect on atmospheric behavior, provide unique problems and possibilities for studying airflow dynamics. A single mountain may be defined

* Corresponding author.

E-mail address: cd210062@student.uthm.edu.my

<https://doi.org/10.37934/sjotfe.5.1.3645a>

differently than a mountainous area or region [1]. A mountain area is typically larger than the sum of individual mountains. Wind in forested mountainous regions differ from those in flat areas due to aerodynamic resistance and topography [2]. These dynamics are especially important in areas where mountain winds have a large influence on human activities and ecosystems [3]. Many of the notable warm and cold periods are found in all-time series and are thus reflective of the whole region. Mountain regions are important sensitive locations with ecological and human systems (e.g., alpine species, valley population density, tourism-based economy) exposed and susceptible to climate change [4]. Air flow in hilly areas is significantly influenced by slopes and valleys [5].

Advances in computational fluid dynamics (CFD) have transformed the study of external airflow in complicated terrains, enabling the simulation of intricate interactions between wind and mountainous topography. Computational fluid dynamics (CFD) is a popular method for simulating microscale wind environments near the surface. It can account for obstructions due to its smaller cell size compared to mesoscale numerical weather modeling and simulate airflow in complicated mountainous areas [6]. An important problem in external airflow analysis is effectively capturing turbulence, which is inherently chaotic and complicated. Various turbulence models are used in CFD simulations to solve this problem [7]. Turbulence models, such as $k-\epsilon$ or $k-\omega$, represent the impact of topographical abnormalities on airflow patterns. These conditions specify how the airflow interacts with the surrounding environment, including wind speed, direction, and temperature gradients [8]. The present research examines the impact of rib configurations on wind pressure on high-rise structures, as well as the impact of roughness on turbulent boundary layer flow over a two-dimensional plunged mountain [9]. Integrating heat transfer analysis into CFD models improves our understanding of thermal interactions in external environments [10].

One of the primary reasons for researching mountain exterior airflow is the growing demand for sustainable energy options. Mountainous regions are frequently recognized as ideal places for wind farms due to their high wind speeds and continuous airflow [11]. However, because of the complicated turbulence and fluctuation of wind conditions, comprehensive models are required to optimize turbine location and assure operating safety [12]. Wind conditions in the constructed environment are complicated, with lower wind speeds and more turbulence due to the presence of barriers [13]. Computational fluid dynamics (CFD) simulation is a cost-effective and energy-efficient way for simulating wind fields over difficult terrain. It also provides comprehensive flow field characteristics [14,15]. The complicated geology of mountainous locations, with changing heights, slopes, and surface roughness, makes it difficult to precisely forecast airflow behavior [16]. Accurate modeling of these interactions is critical for forecasting temperature distributions and improving designs for energy efficiency and thermal comfort [17].

2. Methodology

This chapter describes the methods used to analyze external airflow and heat transfer around a mountainous region using computational fluid dynamics (CFD). The approach focuses on simulating various operating conditions to evaluate the thermal performance and flow behavior of the mountain environment [18]. Key parameters, such as wind velocity, inlet temperature, and mountain surface temperature, are systematically varied to study their effects on heat transfer and airflow dynamics [19]. The computational domain and mountain geometry are designed to replicate real-world topographical features, ensuring the accuracy of the simulation. The use of turbulence models, boundary condition definitions, and high-resolution meshing techniques ensures reliable and consistent results [20]. This organized methodology provides valuable insights into the interaction

between airflow and heat transfer, contributing to a better understanding of thermal and flow behavior in complex natural terrains.

2.1 Geometry

The geometry used for the mountain airflow investigation was represented by detailed views from the top, side, front, and isometric viewpoints as shown in Figure 1. The top view represented the surface contour and size, highlighting the terrain's diverse and uneven features. The side and front views showed elevation fluctuations and general thickness, giving insight into the mountain's vertical characteristics. The isometric view incorporated components from all previous viewpoints to create a three-dimensional perspective, which improved comprehension of the mountain's overall shape. This rich depiction allowed for precise and consistent simulation of external airflow, capturing how wind interacts with the complex topography and contributing to accurate predictions of airflow patterns and temperature distribution.

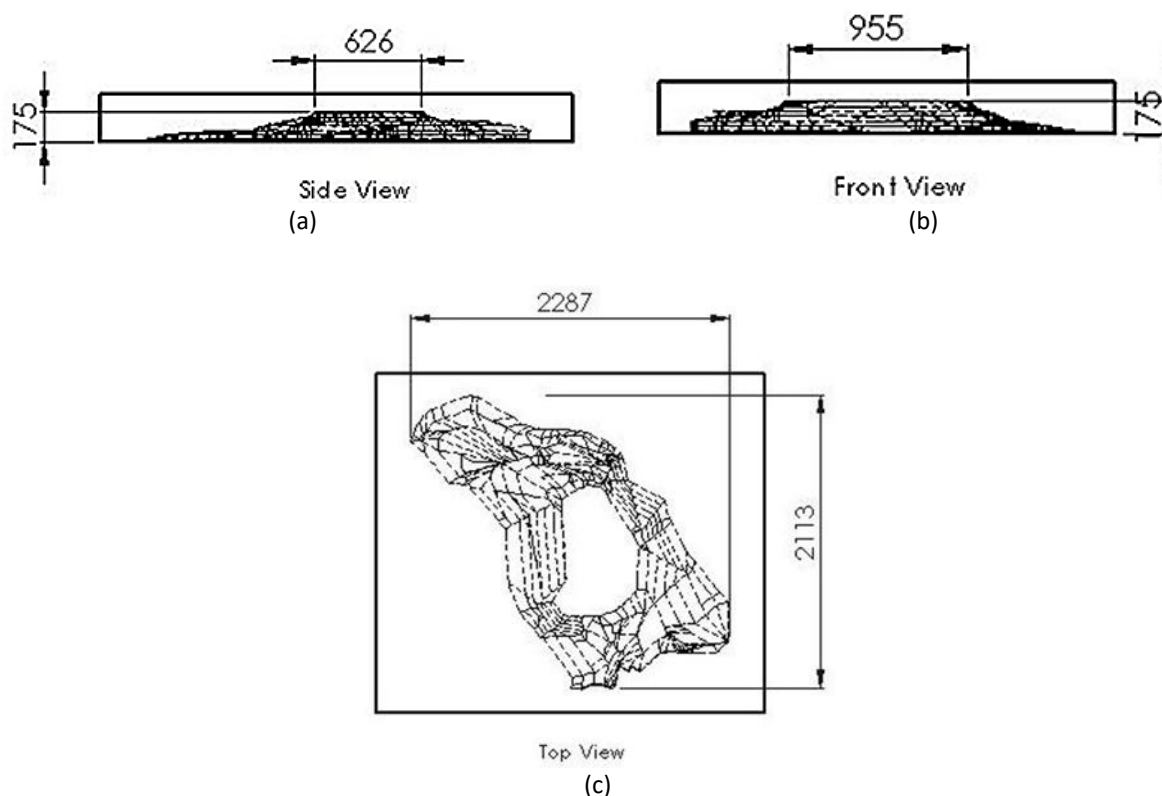


Fig. 1. Geometry of the mountain model (a) Side view (b) Front view (c) Top view

2.2 Discretization of Meshing

Mesh face sizing and the patch-conforming approach were used on the mountainous geometry to ensure the simulation results were precise and reliable as shown in Figure 2. The computational domain was represented by an unstructured mesh with variable element sizes. The grid independence test (GIT) confirmed that mesh size has no major effect on airflow patterns. Four various element sizes were examined, with an emphasis on crucial locations such as the mountain's peaks, valleys, and slopes with strong velocity and pressure gradients. The simulation's final mesh included 1,180,037 elements, indicating that 40 mm element size gave the highest accuracy in

simulating the intricate interplay between wind and mountainous topography. This thorough meshing method resulted in precise airflow analysis over the mountain terrain.

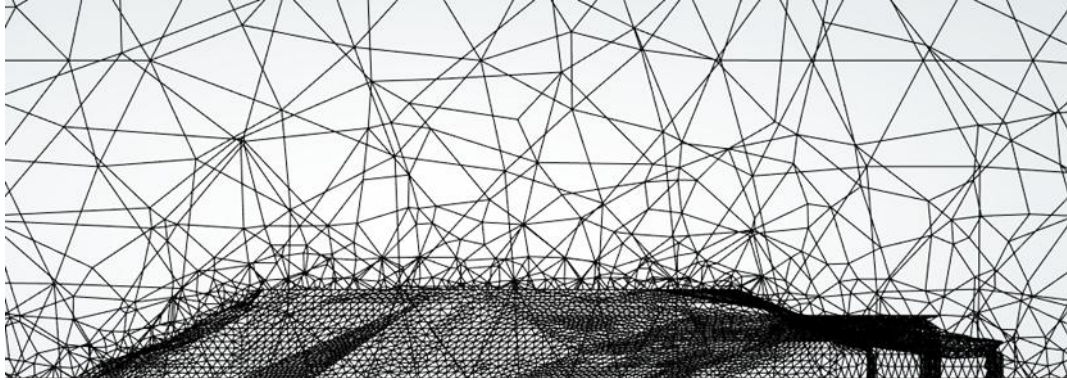


Fig. 2. Face sizing meshing on the surface of the mountain

2.3 Governing Equation

The governing equations for this project, focusing on external airflow and heat transfer around a mountain, are based on the principles of mass, momentum, and energy conservation. These equations describe the interaction of airflow with the mountain surface and the resulting thermal behavior. The continuity equation ensures mass conservation in the airflow, while the momentum equation accounts for forces acting on the fluid, such as pressure gradients, inertial forces, and viscous effects. The energy equation governs heat transfer between the heated mountain surface and the surrounding airflow. The equations, derived from the Navier-Stokes framework for incompressible flows, are as follows:

$$\text{Continuity equation (mass conservation): } \frac{\partial u}{\partial x} + \frac{\partial v}{\partial y} + \frac{\partial w}{\partial z} = 0 \quad (1)$$

For incompressible flow ($\rho=\text{constant}$), this reduces to:

$$\nabla \cdot \mathbf{v} = 0 \quad (2)$$

Momentum equation (Navier-Stokes):

$$\frac{\partial(\rho \mathbf{v})}{\partial t} + \nabla \cdot (\rho \mathbf{v} \otimes \mathbf{v}) = -\nabla P + \mu \nabla^2 \mathbf{v} + \rho \mathbf{g} \quad (3)$$

where \mathbf{v} is velocity vector, P is pressure, μ dynamic viscosity and \mathbf{g} is gravitational acceleration vector.

$$\text{Energy equation (heat transfer): } \frac{\partial(\rho E)}{\partial t} + \nabla \cdot [\mathbf{v}(\rho E + P)] = \nabla \cdot (k \nabla T) + \Phi \quad (4)$$

where $E = e + \frac{1}{2} |\mathbf{v}|^2$ is total energy per unit mass (internal energy e + kinetic energy), T is temperature, k is thermal conductivity and Φ is viscous dissipation term. These equations are numerically solved using CFD techniques in ANSYS Fluent, considering the boundary conditions specific to the mountain environment. The no-slip condition is applied at the mountain surface, where airflow velocity is zero, while thermal boundary conditions include a constant surface

temperature of 1200°C. At the domain inlet, velocity and temperature are specified, and at the outlet, a pressure outlet condition is applied. These governing equations provide the foundation for simulating airflow dynamics and heat transfer behavior around the mountain terrain.

2.4 Boundary Condition Parameters

For the simulation of mountain external airflow considering heat transfer, the following boundary conditions are applied as shown in Figure 3. The inlet velocity varies based on the wind conditions: for high velocity, the inlet velocity is 150 m/s with a temperature of 25°C, for medium velocity, it is 100 m/s with a temperature of 25°C, and for low velocity, it is 50 m/s with a temperature of 25°C. The mountain surface maintains a constant temperature of 1200°C across all cases. At the outlet, the backflow temperature is set to 35°C. The airflow approaches the mountain at an angle of 0° to analyse flow separation, turbulence formation, and heat transfer. A pressure outlet condition is applied at the domain outlet, ensuring smooth airflow exit at atmospheric pressure. The mountain surface follows a no-slip boundary condition where the airflow velocity at the surface is zero, accurately capturing frictional effects and convective heat transfer. To optimize computational efficiency while maintaining accuracy, the lateral boundaries of the computational domain are treated as symmetry planes.

Additionally, the k- ϵ , k- ω , and k-kl- ω turbulence models are employed to evaluate turbulent flow behaviours, including recirculation zones and boundary layer interactions around the mountain. These boundary conditions ensure realistic modelling of aerodynamic and thermal interactions between the external airflow and the mountain environment.

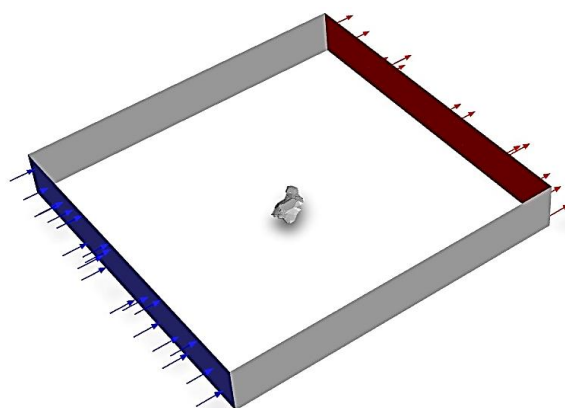


Fig. 3. Boundary condition of mountain model

3. Results

Various turbulence models are used to study external airflow over the mountainous terrain at varying wind velocities. Flow properties, such as separation and vortex generation, are investigated using turbulence models from the simulations. The study sheds light on how the mountain's diverse geography impacts airflow patterns, as well as contributing to our knowledge of microclimates and their consequences on the surrounding ecosystem.

3.1 Temperature Distribution

The temperature distribution analysis demonstrates how the external airflow of the mountainous region responds to different wind velocities and highlights the influence of various turbulence models

in predicting accurate temperature fields. Three turbulence models, namely K-epsilon, k-omega SST, and k-kl-omega were employed in the simulations to capture the complex airflow interactions with the mountain's topography. These models provided detailed insights into the temperature distribution patterns, enabling a better understanding of the thermal behavior under different wind conditions. The analysis also underscores the importance of selecting appropriate turbulence models to ensure the precision and reliability of simulation results, particularly in regions with intricate terrain and varying climatic conditions.

3.1.1 K-Epsilon Model

The temperature distribution results show in Figure 4. demonstrate the influence of airflow velocity on heat dissipation and surface temperature around a mountain model using the k-epsilon turbulence model. At low velocity (50 m/s), the heat distribution appears concentrated near the surface, indicating limited cooling effects. As velocity increases to medium (100 m/s), heat dissipation becomes more prominent, spreading further outward due to stronger convective effects. At high velocity (150 m/s), the temperature gradient is significantly reduced, suggesting enhanced cooling efficiency with faster airflow. This analysis highlights the critical role of airflow velocity in regulating temperature distribution in external airflow scenarios.

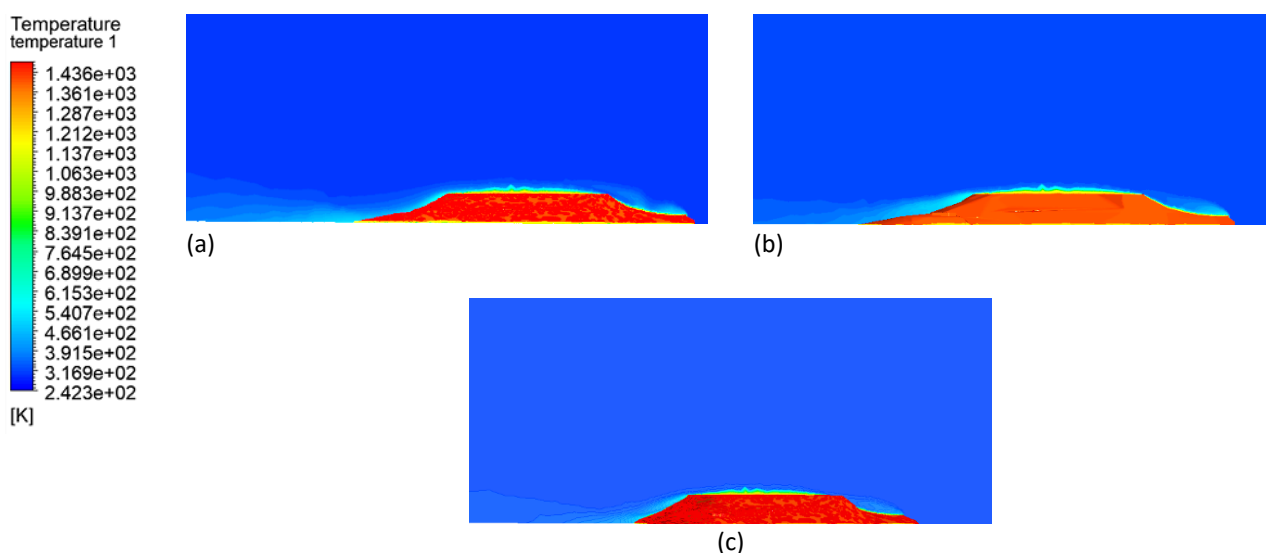


Fig. 4. Temperature distribution across k-epsilon model (a) Low velocity (50 m/s) (b) Medium velocity (100 m/s) (c) High velocity (150 m/s)

3.1.2 K-omega SST model

The temperature distribution for the k-omega SST model, as shown in Figure 5, demonstrates a similar trend to the k-epsilon model, but with greater stability and smoother gradients. At low velocity (50 m/s), heat is retained close to the surface, resulting in higher localized temperatures. At medium velocity (100 m/s), the heat begins to spread further outward due to enhanced convective effects, though the temperature distribution appears more balanced compared to the k-epsilon model. At high velocity (150 m/s), the temperature gradients are more uniform, with effective cooling observed across the entire domain. This suggests that the k-omega SST model better captures the transition between flow regions and provides more accurate predictions for heat transfer in complex mountain airflow scenarios.

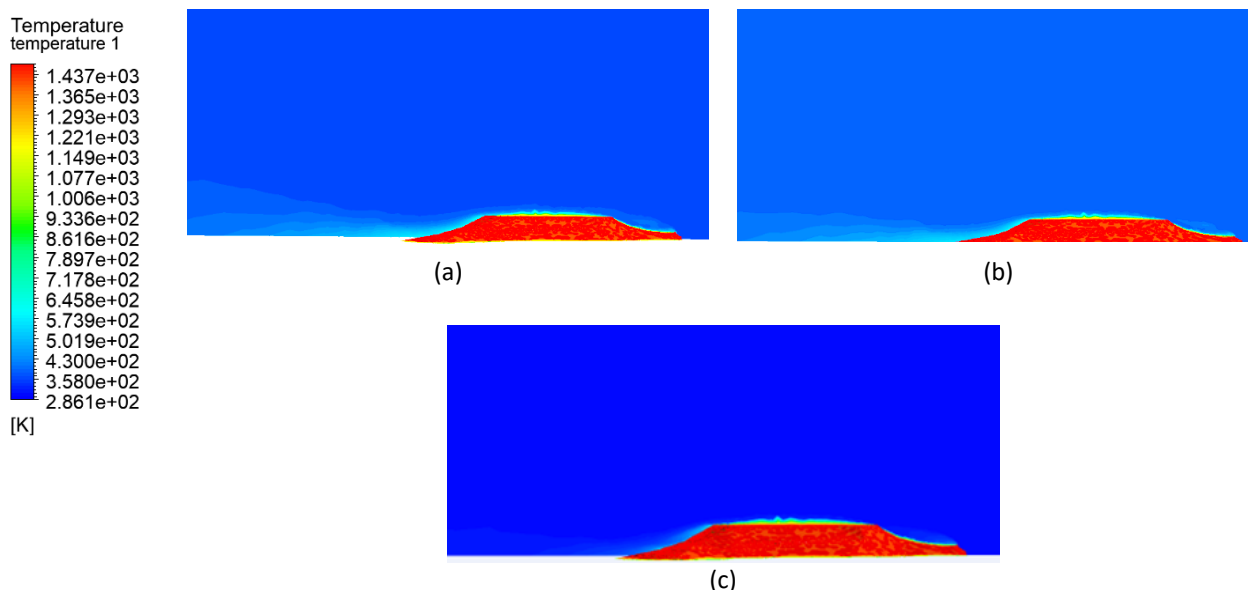


Fig. 5. Temperature distribution across k-omega SST model (a) Low velocity (50 m/s) (b) Medium velocity (100 m/s) (c) High velocity (150 m/s)

3.1.3 Effect of angle of attack

The temperature distribution across the K-KL-Omega model, as shown in Figure 6, highlights the influence of varying velocities on thermal behavior. At low velocity (50 m/s), the temperature field shows limited diffusion, with heat concentrating near the heated surface. At medium velocity (100 m/s), the thermal profile expands slightly, indicating enhanced heat transfer due to increased convection. Finally, at high velocity (150 m/s), the temperature distribution exhibits significant dispersion, suggesting efficient heat removal and more uniform cooling over the surface. These results underscore the strong correlation between flow velocity and thermal performance in the K-KL-Omega model, emphasizing its role in optimizing heat transfer.

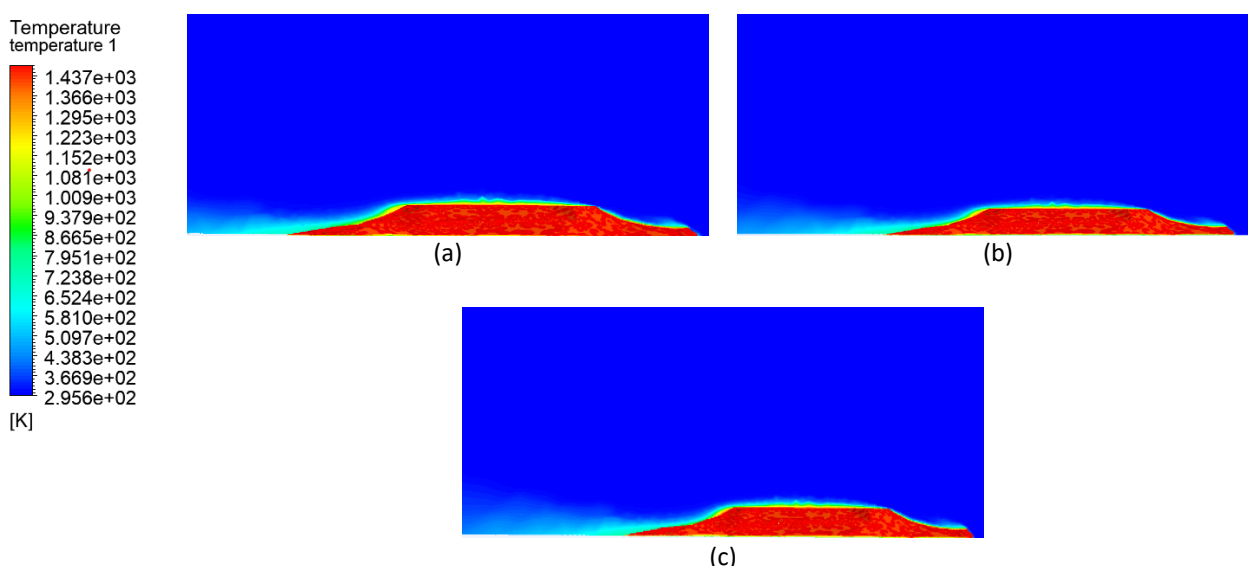


Fig. 6. Temperature distribution across k-kl-omega model (a) Low velocity (50 m/s) (b) Medium velocity (100 m/s) (c) High velocity (150 m/s)

3.1.4 Average temperature distribution

Table 1 shows the average temperature on the mountain surface at various wind speeds for three turbulence models: k-epsilon, k-omega SST, and k-kl-omega. The temperature distribution analysis investigates how the mountain's external airflow behaves under varying wind velocities and highlights the impact of different turbulence models on temperature field predictions. The graph in Figure 7 shows the relationship between wind velocity (in meters per second) and the average temperature of the mountain surface (in degrees Celsius) for three turbulence models: K-epsilon, K-omega SST, and K-kl-omega. The K-epsilon model shows a higher average temperature that slightly increases with wind velocity. The K-omega SST model maintains a relatively constant temperature across varying wind speeds. The K-kl-omega model displays a temperature trend similar to K-omega SST, with slight variations. This graph demonstrates how different turbulence models predict the mountain surface temperature under varying wind conditions, highlighting the importance of model selection for accurate simulation results.

Table 1

Average temperature on the mountain surface in different velocity across turbulence models

Velocity of wind (m/s)	Average temperature of the mountain surface		
	K-epsilon	K-omega SST	K-kl-omega
50	25.7827	25.276816	25.25315
100	25.843024	25.248061	25.22737
150	25.881695	25.245751	25.22559

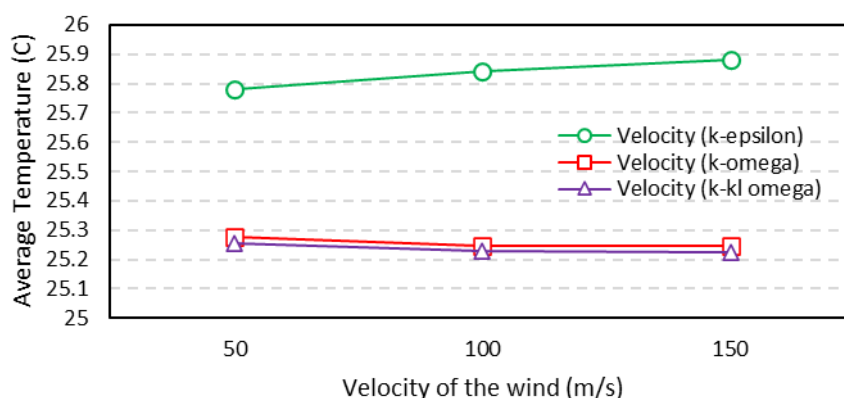


Fig. 7. Average temperature of the mountain surface

3.2 Grid Independence Test (GIT)

Table 2 shows the grid independence test (GIT) results for various mesh element sizes. The test showed that mesh size has no significant impact on airflow patterns, confirming the accuracy and trustworthiness of simulation results for mountain airflow research. Four distinct element sizes were examined, each focused on crucial places such as mountain peaks, valleys, and slopes with strong velocity and pressure gradients. The final mesh, with the appropriate element size, achieved the highest accuracy in modeling the intricate interactions between wind and mountainous topography. This thorough meshing method allows precise airflow analysis and reliable temperature distribution predictions, hence confirming the specified turbulence models.

Table 2
Comparison between element size

Element size (mm)	No. of elements	Average element quality	Average temperature
100	289635	0.700489	1198.1527
80	395321	0.700798	1198.4032
60	622246	0.699978	1199.7539
40	1180037	0.6992701	1200.0221

4. Conclusions

This study successfully used computational fluid dynamics (CFD) to model external airflow and heat transfer across a slope, offering important insights into the impacts of wind velocity and turbulence models on temperature distribution and flow behavior. The findings highlight the necessity of choosing adequate simulation parameters to make accurate forecasts, which have practical implications in renewable energy optimization, environmental research, and climate modeling. To build on this work, it is recommended that the simulation results be validated with experimental data for increased reliability, that the findings be generalized across a wider range of environmental conditions, and that these insights be integrated into wind energy systems for improved turbine placement and efficiency.

References

- [1] Ramasamy, P., S. S. Chandel, and Amit Kumar Yadav. "Wind speed prediction in the mountainous region of India using an artificial neural network model." *Renewable Energy* 80 (2015): 338-347. <https://doi.org/10.1016/j.renene.2015.02.034>
- [2] Ha, Taehwan, In-bok Lee, Se-Woon Hong, and Kyeong-Seok Kwon. "CFD assisted method for locating and processing data from wind monitoring systems in forested mountainous regions." *Biosystems Engineering* 187 (2019): 21-38. <https://doi.org/10.1016/j.biosystemseng.2019.08.012>
- [3] Trentmann, Jörg, Christian Keil, Marc Salzmann, Christian Barthlott, H-S. Bauer, T. Schwitalla, M. G. Lawrence, D. Leuenberger, V. Wulfmeyer, U. Corsmeier, C. Kottmeier and H. Wernli "Multi-model simulations of a convective situation in low-mountain terrain in central Europe." *Meteorology and Atmospheric Physics* 103 (2009): 95-103. <https://doi.org/10.1007/s00703-008-0323-6>
- [4] Terzi, Stefano, Silvia Torresan, Stefan Schneiderbauer, Andrea Critto, Marc Zebisch, and Antonio Marcomini. "Multi-risk assessment in mountain regions: A review of modelling approaches for climate change adaptation." *Journal of environmental management* 232 (2019): 759-771. <https://doi.org/10.1016/j.jenvman.2018.11.100>
- [5] Ha, Taehwan, In-bok Lee, Kyeong-seok Kwon, and Seung-Jae Lee. "Development of a micro-scale CFD model to predict wind environment on mountainous terrain." *Computers and Electronics in Agriculture* 149 (2018): 110-120. <https://doi.org/10.1016/j.compag.2017.10.014>
- [6] Jiang, Xue, Hao Yang, Guanming Lin, Wenyi Dang, Anfeng Yu, Jiedong Zhang, Meng Gu, and Chuntao Ge. "Measurements and predictions of harmful releases of the gathering station over the mountainous terrain." *Journal of Loss Prevention in the Process Industries* 71 (2021): 104485. <https://doi.org/10.1016/j.jlp.2021.104485>
- [7] Kummitha, Obula Reddy, R. Vijay Kumar, and V. Murali Krishna. "CFD analysis for airflow distribution of a conventional building plan for different wind directions." *Journal of Computational Design and Engineering* 8, no. 2 (2021): 559-569. <https://doi.org/10.1093/jcde/qwaa095>
- [8] Kato, Shinsuke. "Review of airflow and transport analysis in building using CFD and network model." *Japan Architectural Review* 1, no. 3 (2018): 299-309. <https://doi.org/10.1002/2475-8876.12051>
- [9] Alavi, Fatemesadat, Ali Akbar Moosavi, Abdolmajid Sameni, and Mohammadamin Nematollahi. "Numerical simulation of wind flow characteristics over a large-scale complex terrain: A computational fluid dynamics (CFD) approach." *City and Environment Interactions* 22 (2024): 100142. <https://doi.org/10.1016/j.cacint.2024.100142>
- [10] Jiru, Teshome Edae, and Girma Tsegaye Bitsuamlak. "Application of CFD in modelling wind-induced natural ventilation of buildings-A review." *International Journal of Ventilation* 9, no. 2 (2010): 131-147. <https://doi.org/10.1080/14733315.2010.11683875>
- [11] Lei, Ma, Luan Shiyan, Jiang Chuanwen, Liu Hongling, and Zhang Yan. "A review on the forecasting of wind speed and generated power." *Renewable and Sustainable Energy Reviews* 13, no. 4 (2009): 915-920. <https://doi.org/10.1016/j.rser.2008.02.002>

- [12] Feng, Ju, Wen Zhong Shen, and Ye Li. "An optimization framework for wind farm design in complex terrain." *Applied Sciences* 8, no. 11 (2018): 2053. <https://doi.org/10.3390/app8112053>
- [13] Anup, K. C., Jonathan Whale, and Tania Urmee. "Urban wind conditions and small wind turbines in the built environment: A review." *Renewable Energy* 131 (2019): 268-283. <https://doi.org/10.1016/j.renene.2018.07.050>
- [14] Huang, Guoqing, Xu Cheng, Liuliu Peng, and Mingshui Li. "Aerodynamic shape of transition curve for truncated mountainous terrain model in wind field simulation." *Journal of Wind Engineering and Industrial Aerodynamics* 178 (2018): 80-90. <https://doi.org/10.1016/j.jweia.2018.05.008>
- [15] Maza, J., and G. Nicoletti. "CFD-rans applications in complex terrain analysis. Numerical vs experimental results a case study: Cuzzovalefondi wind farm in sicily." *Delta* 5 (2006): 10.
- [16] Huo, Hongyuan, Fei Chen, Xiaowei Geng, Jing Tao, Zhansheng Liu, Wenzhi Zhang, and Pei Leng. "Simulation of the urban space thermal environment based on computational fluid dynamics: A comprehensive review." *Sensors* 21, no. 20 (2021): 6898. <https://doi.org/10.3390/s21206898>
- [17] Awungabeh, Flavis Akawung, John Ebot Besong, and Fujimoto Yasutaka. "Airflow cooling mechanism for high-power-density surface mounted permanent magnet motor." *Authorea Preprints* (2024). <https://doi.org/10.36227/techrxiv.23812866.v1>
- [18] Yadav, Anshul, Chandra Prakash Singh, Raj Vardhan Patel, Pawan Kumar Labhasetwar, and Vinod Kumar Shahi. "Computational fluid dynamics based numerical simulations of heat transfer, fluid flow and mass transfer in vacuum membrane distillation process." *Water Supply* 22, no. 7 (2022): 6262-6280. <https://doi.org/10.2166/ws.2022.200>
- [19] Ye, Yu, Xunjian Xu, Li Yang, and Yusheng Yi. "Research on terrain aerodynamics analysis of power grid structure at different temperature." In *E3S Web of Conferences*, vol. 260, p. 02010. EDP Sciences, 2021. <https://doi.org/10.1051/e3sconf/202126002010>
- [20] Li, Ruige, Yanru Wang, Hongjian Lin, Hai Du, Chunling Wang, Xiaosu Chen, and Mingfeng Huang. "A mesoscale CFD simulation study of basic wind pressure in complex terrain—A case study of Taizhou City." *Applied Sciences* 12, no. 20 (2022): 10481. <https://doi.org/10.3390/app122010481>